

# Enhanced cooperativity below the caging temperature of glass-forming liquids

B. M. ERWIN<sup>1</sup>, R. H. COLBY<sup>1(\*)</sup>, S. Y. KAMATH<sup>1</sup> and S. K. KUMAR<sup>2</sup>

<sup>1</sup> *Department of Materials Science and Engineering and the Materials Research Institute  
The Pennsylvania State University - University Park, PA 16802, USA*

<sup>2</sup> *Department of Chemical and Biological Engineering, Rensselaer Polytechnic Institute  
- Troy, NY 12180, USA*

PACS. 64.70.Pf – Glass transitions.

PACS. 61.43.Fs – Glasses.

PACS. 61.20.Lc – Time-dependent properties; relaxation.

**Abstract.** – The utility of a cooperative length scale for describing the dynamics of small molecule glass-formers is shown. Molecular Dynamics and Monte Carlo simulations reveal a distribution of cooperatively moving fractal events below the temperature  $T_A$  at which dynamics become caged. Guided by these results, four straightforward methods emerge to recognize  $T_A$  in experimental data and quantify the length scale that grows on cooling below  $T_A$ . This length scale is consistent with 4-D NMR experiments which are sensitive to the slow moving population.

Many liquids either cannot crystallize or crystallize sufficiently slowly that they vitrify below their glass transition temperature  $T_g$ . A fundamental understanding of glass formation is still lacking because it has not been firmly established whether the pronounced slowing down is simply kinetic in origin or there is an underlying thermodynamic character [1–6]. This letter shows that there is a natural length scale for cooperative motion that grows as the glass transition is approached.

The 1965 model of Adam and Gibbs [1] suggests that there should be cooperative motion in glass-forming liquids. The size  $\xi$  of the cooperative volume is related to the configurational entropy of the liquid  $S_c$ . At temperatures  $T$ , sufficiently above  $T_g$ , where the relaxation time  $\tau_\alpha$ , and the viscosity  $\eta$ , vary as  $\tau_\alpha \sim \eta/T \sim \exp[E/k_B T]$ , all molecules undergo independent local Brownian movements without signs of cooperativity. As temperature is lowered, the density of the liquid gradually increases and Brownian motion becomes hindered, as neighboring particles block each others attempts to move. This crowding leads to *cooperative dynamics* [5–9], active for all  $T$  below the *caging temperature*  $T_A$ . The onset of cooperativity is also accompanied by the observed ‘caging effect’ in the mean-square displacement of a particle between the ballistic and self-diffusive regimes, and a reduction in  $S_c$ , causing  $\xi$  to grow. These changes result in a progressively stronger temperature dependence of  $\eta$  and  $\tau_\alpha$  at lower temperatures.

---

(\*) E-mail: [rhc@plmsc.psu.edu](mailto:rhc@plmsc.psu.edu)

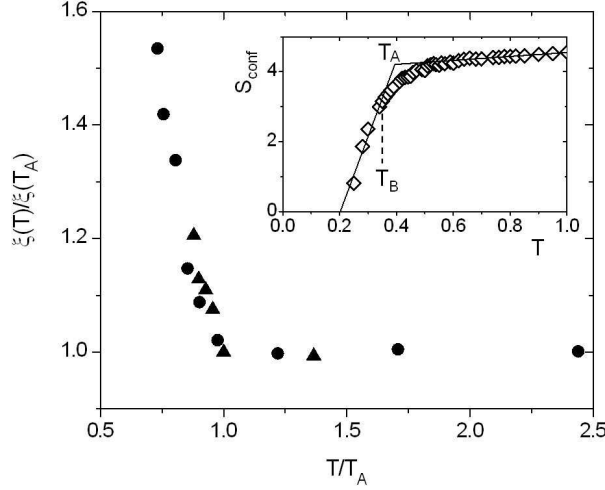


Fig. 1 – Simulation results for the length scale of cooperative motion as a function of reduced temperature. From molecular dynamics simulations of Lennard-Jones sphere mixtures ( $\blacktriangle$  [11]) and from Monte Carlo simulations of the bond fluctuation model at density 0.8 for chains of 10 monomers ( $\bullet$  [18]). Inset is the temperature dependence of the configurational entropy for chains of 10 monomers ( $\diamond$  [10]).

Since experimental attempts to identify the length scale for cooperative motion have met with limited success [2–4], the dominant evidence for this quantity is from computer simulations [8–17]. Simulations have the profound advantages of direct observation of motion and straightforward identification of both the *size and shape* of cooperatively rearranged regions. Equilibrium simulations of liquids are not yet possible near  $T_g$ , but have been done down to  $0.7T_A$  [10]. In addition to confirming the essential aspects of the Adam and Gibbs model, simulations have provided two novel insights. Instead of a single size scale for cooperative motion, there is in fact a *broad distribution of size scales* below  $T_A$  [8, 12–19]. The largest size in this distribution  $\xi$  grows rapidly as temperature is lowered, as expected by Adam and Gibbs [1]. The second important observation is that the cooperatively rearranging regions are not the three-dimensional volumes that were initially proposed, but instead are *fractal* [8, 15–18]. The observed fractal dimension (of order 2) clearly shows that the majority of molecules within the volume  $\xi^3$  have *not* participated in the cooperative motion. Consequently, a new model for cooperative motion was proposed that accommodates these new insights [20]. All glass-forming liquids show a temperature dependence of cooperative size scale, with commensurate effects in viscosity and relaxation time, in reasonable accord with the expectation of dynamic scaling [20, 21] in the temperature range  $T_C < T < T_A$ .

$$\xi^6 \sim \tau_\alpha e^{-E_\alpha/k_B T} \sim \eta e^{-E_\eta/k_B T} \sim (T - T_C)^{-9} \quad (1)$$

The critical temperature  $T_C$ , is slightly *below*  $T_g$  and is the temperature at which the *equilibrium* extrapolated values of  $\xi$ ,  $\tau_\alpha$  and  $\eta$  all diverge. The material-specific activation energy apparently depends on whether segmental relaxation ( $E_\alpha$ ) or viscosity ( $E_\eta$ ) is measured, with  $E_\eta/E_\alpha \simeq 1.2$  for non-polymeric organic glasses.

Figure 1 shows data for  $\xi$  as obtained from Molecular Dynamics simulations [8] and new results from Monte Carlo (MC) simulations on the bond fluctuation model [10]. In the MC simulations the mobile particles are identified as those that move over a time scale of interest.

TABLE I – Temperatures and length scales for five glass-forming liquids. All  $T_g$  are from Böhmer, *et al.* [28] with the exception PDE where  $T_g = T(\tau_\alpha = 100 \text{ sec})$ . All  $T_B$  are the crossover temperature between Vogel-Fulcher fits with the exception of D-sorbitol [29] and glycerol [4] from  $\alpha\beta$ -merging.

Property	$T_A$ [K]	$T_B$ [K]	$T_g$ [K]	$T_C$ [K]	$r_{vdW}$ [Å]	$\xi(T_A)$ [Å]	$\xi(T_g)$ [Å]	References
PDE	355	325	294	278	4.1			[22, 30–32]
D-sorbitol	350	335	274	257	3.4	$3.8 \pm 1.8$	$27. \pm 13.$	[33–35]
OTP	315	290	241	227	3.7	$3.5 \pm 1.0$	$52. \pm 18.$	[30, 31, 36–41]
salol	275	265	218	204	3.5			[22, 30–32]
glycerol	280	262	190	173	2.7	$1.9 \pm 0.8$	$25. \pm 11.$	[30, 31, 40–42]

We then look for clusters of these mobile particles and find that their sizes are a function of time for short times, but quickly become time independent up to  $\tau_\alpha$ . We only consider cluster sizes in this intermediate time range. Figure 1 shows mean sizes of the mobile particle clusters as a function of  $T$ . Both sets of simulations show that  $\xi$  is sensibly independent of temperature above  $T_A$ , but then grows rapidly when temperature is lowered below  $T_A$ . The very different nature of the simulations used for the data in Fig. 1 strongly points to the existence of a growing length scale below at  $T < T_A$ . The inset of Fig. 1 shows that  $S_c$  as defined by Adam and Gibbs also changes character at  $T_A$  with a broad crossover between  $T_B$  [22] below which Eq. 1 or Vogel-Fulcher should describe dynamics and a much higher temperature above which dynamics are Arrhenius [22].

Guided by simulations, and owing to the abrupt change in the very nature of relaxation at  $T_A$  [9, 10, 23–25], the caging temperature is easily identified by a variety of experiments probing liquid dynamics. We demonstrate this point with four dynamics experiments that have broad dynamic range: rotation and translational diffusion of molecular probes, self-diffusion, dielectric spectroscopy and rheology. Molecular probe and self-diffusion techniques are particularly noteworthy because they provide a *model independent* measure of  $T_A$ . The length scales extracted from these experiments, which are in *quantitative* agreement with existing  $\xi(T)$  data from 4-D NMR [26, 27], show a strong temperature dependence *only below*  $T_A$ .

$T_C$  is determined by using literature data on  $\tau_\alpha$  and  $\eta$  well below  $T_A$  for glycerol, *o*-terphenyl (OTP), phenolphthaleinedimethylether (PDE), salol and D-sorbitol and fitting them to Eq. 1 (Table I).  $T_A$  is defined from the crossovers in Fig. 2. Different dynamic experiments provide consistent determinations of both  $T_A$  and  $T_C$ . Table I also reports the crossover temperature  $T_B$  from Donth [4] where dynamics switch from one Vogel-Fulcher form to another [22].  $T_B$  is typically about 20 K below  $T_A$  and corresponds to the upper temperature limit where dynamic scaling or Vogel-Fulcher quantitatively describe the temperature dependence of dynamics.

The Stokes-Einstein relation expects the rotational relaxation time  $\langle\tau_r\rangle$  and translational diffusion coefficient  $D_t$  of probe molecules are coupled so that their product is independent of temperature. Above  $T_A$  the probes diffuse a distance of order their own size in the time it takes for the probe to rotate. However, at  $T_A$  these two dynamics *decouple*, a fact which can be used to establish a length scale. To understand this, consider a bimodal distribution of  $\phi_f$  fast and  $\phi_s = 1 - \phi_f$  slow particles. The average rotational time is dominated by the slow particles

$$\langle\tau_r\rangle = \phi_s\tau_s + \phi_f\tau_f \cong \phi_s\tau_s \quad (2)$$

since  $\phi_s \gg \phi_f$  and  $\tau_s \gg \tau_f$ . The diffusion coefficient is the sum of fast and slow contributions

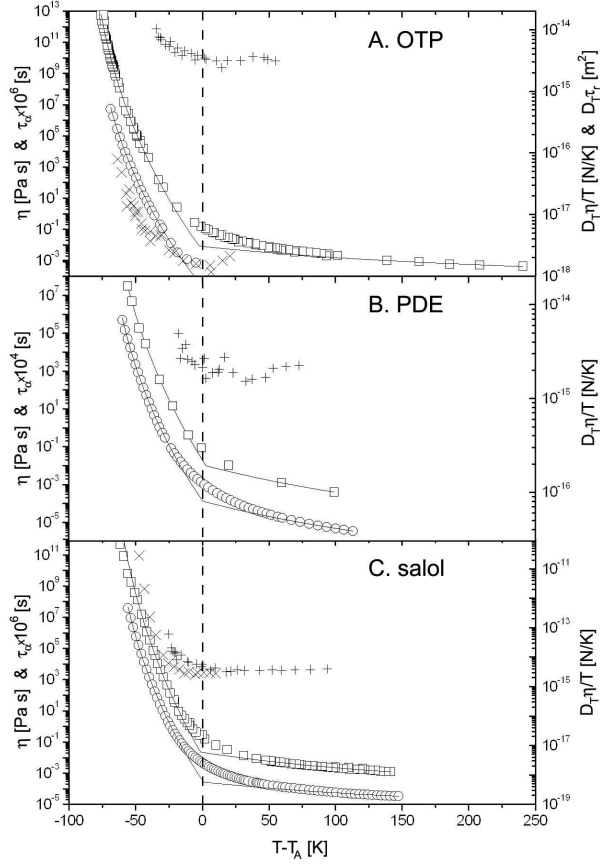


Fig. 2 – Dynamic data for OTP, PDE and salol above and below  $T_A$ . Temperature dependence of viscosity ( $\square$ ),  $\tau_\alpha$  ( $\circ$ ), probe diffusion ( $\times$ ) and self-diffusion ( $+$ ). Solid curves are fits of Eq. 1 to data below  $T_A$  and Arrhenius fits to data above  $T_A$  for both viscosity and dielectric data. The dashed line is  $T_A$  taken from the extrapolation of dynamic scaling to the Arrhenius temperature dependence of viscosity from high- $T$ . See Table I for references.

$$D_t = \phi_s D_s + \phi_f D_f = \phi_s \xi_s^2 / 6\tau_s + \phi_f \xi_f^2 / 6\tau_f \quad (3)$$

where  $\xi_s^2 \equiv 6D_s\tau_s$  and  $\xi_f^2 \equiv 6D_f\tau_f$ . Since  $\phi_s \approx 1$ , the product  $6D_t\langle\tau_r\rangle \cong \phi_s^2\xi_s^2 + \phi_f\phi_s\xi_f^2\tau_s/\tau_f$  can be used to define a length scale,

$$\xi \cong \xi_s = \sqrt{6D_t\langle\tau_r\rangle}. \quad (4)$$

Fig. 3.A shows the temperature dependence of this length scale for OTP and it *quantitatively* agrees with 4-D NMR, which is known to target the slow contribution  $\xi_s$ . Hence,  $\phi_s^2\xi_s^2 \gg \phi_f\phi_s\xi_f^2\tau_s/\tau_f$ , justifying Eq. 4.

In the calculation of  $\xi$ ,  $\langle\tau_r\rangle$  was interpolated [43] using the temperature dependence of viscosity from various sources [37, 40, 41]. In OTP,  $\xi$  of anthracene (filled circles in Fig. 3.A) shows a strong temperature dependence over the entire experimental temperature range because all  $T < T_A$ , whereas the larger tetracene probe (filled triangles in Fig. 3.A) is clearly temperature dependent below  $T_A$  and independent of temperature above  $T_A$ .

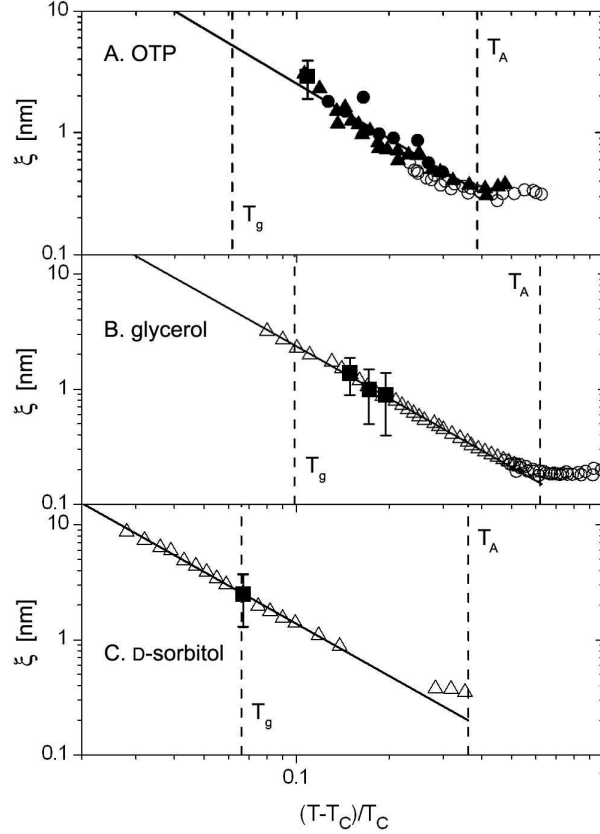


Fig. 3 – The temperature dependence of the cooperative length of OTP, glycerol and D-sorbitol. Filled symbols denote absolute measures of  $\xi$  from 4-D NMR (■ with error bars [27]) and calculations using probe dynamics (● anthracene [36]; ▲ tetracene [36]). Open symbols denote measures of the temperature dependence of  $\xi$  from self-diffusion (○ [30, 38]) and dielectric measurements (△ [31, 34]) which have been vertically shifted into agreement with the absolute measures of  $\xi$ . Dashed lines denote  $T_A$  and  $T_g$  (values in Table I). The solid line is the slope of  $-3/2$  expected by dynamic scaling (Eq. 1).

$T_A$  is the temperature below which  $\xi$  becomes temperature dependent. Cooperativity causes the breakdown of the Stokes-Einstein relation, as is made evident when  $D_t\eta/T$  becomes temperature dependent at temperatures below  $T_A$  (Fig. 2).

Ideally a probe molecule would have the same shape, size, polarity and properties as the liquid matrix in which it was inserted.  $^1\text{H}$ -NMR can provide measurements of translational and rotational *self*-diffusion coefficients [38]. This allows for direct measurement of  $\xi$  using Eq. 4. Although measurements of  $\langle\tau_r\rangle$  exist [38], they are rare. In the case where measurements of  $\langle\tau_r\rangle$  are lacking, we assume that  $\eta/T$  properly describes the temperature dependence of  $\langle\tau_r\rangle$  [38]. This assumption allows for measurements of  $T_A$  that stand in agreement with the other measurements of  $T_A$ , but with the limitation of not being able to give an absolute measure of  $\xi$ . Each of the glass-formers in Figure 2 show that  $T_A$  measured using dielectric and viscosity data occurs at the same temperature as the breakdown in the Stokes-Einstein relation for self-diffusion standing in agreement with the small probe data.

In Fig. 3.A, the  $\xi$  of OTP from self-diffusion measurements are plotted along with the absolute measurements of  $\xi$  provided by 4-D NMR ( $\xi(252K) = 2.9 \pm 1$  nm, [26]). While each technique measures  $\xi$  differently, they *all stand in quantitative agreement*. The  $\xi$  from self-diffusion data also shows qualitative agreement with the molecular probe data. While  $T_A$  has been determined by applying dynamic scaling to viscosity and dielectric measurements, results from probe molecules and self-diffusion data are in agreement since  $\xi$  becomes temperature-independent above  $T_A$ .

Equation 1 can be used to estimate  $\xi$  from  $\eta$  or  $\tau_\alpha$ , since  $T_C$ ,  $E_\alpha$  and  $E_\eta$  have been previously established by fitting Eq. 1 to data.

$$\xi \sim \tau_\alpha^{1/6} e^{-E_\alpha/6k_B T} \quad T_C < T < T_A \quad (5)$$

In Figs. 3.B and 3.C, dielectric data have been used to plot  $\xi$  of glycerol and D-sorbitol along with measurements from 4-D NMR and in the case of glycerol, self-diffusion.  $\xi$  from dielectric and self-diffusion data were vertically shifted into agreement with  $\xi$  from the absolute measurements that have been provided by 4-D NMR. The resulting data obey the slope of  $-3/2$  expected by dynamic scaling (Eq. 1). The  $\xi$  plotted in Figures 3.B and 3.C shows a clear temperature dependence below  $T_A$ .

$\xi(T_A)$  and  $\xi(T_g)$  are determined from Fig. 3 and listed in Table I. Uncertainty in the measurement of  $\xi$  by 4-D NMR is extrapolated to  $T_A$  and  $T_g$  in cases where 4-D NMR provides the only absolute measure of  $\xi$  used in the determination of  $\xi$ , as is the case with glycerol and D-sorbitol. The van der Waals sphere radii  $r_{vdW}$  of each of the glasses was calculated from atomic radii using the procedures of Edward [44] and are included in Table I. The  $r_{vdW}$  for D-sorbitol, OTP and glycerol are all within the calculated range of  $\xi(T_A)$ , suggesting that the magnitudes of cooperative size calculated herein are reasonable.

Four robust experimental methods for determining the caging temperature have been identified. Of these methods, estimation of the length scale for cooperative motion is best done from measurements of probe diffusion and rotation. However, this has only been done for a select few glass-formers. Far more convenient techniques of dielectric spectroscopy and rheology can determine the *temperature dependence* of the length scale.

Despite the fact that the cooperative volume is fractal instead of space-filling, the essential features of the Adam-Gibbs model [1] are correct. The cooperative size does indeed grow rapidly as temperature is lowered below the caging temperature. Over a temperature range extending from  $T_A$  to  $T_g$ ,  $\xi$  has been observed to increase by an order of magnitude from the van der Waals radius of each molecule, making the insight of Adam and Gibbs particularly noteworthy.

We thank the National Science Foundation (DMR-9977928 and DMR-0422079) for funding.

## REFERENCES

- [1] ADAM G. and GIBBS J., *J. Chem. Phys.*, **43** (1965) 139.
- [2] SILLESCU H., *J. Non-Cryst. Solids*, **243** (1999) 81.
- [3] EDIGER M., *Annu. Rev. Phys. Chem.*, **51** (2000) 99.
- [4] DONTN E., *The glass transition: relaxation dynamics in liquids and disordered materials* (Springer, New York) 2001.
- [5] KOB W., *J. Phys. Condens. Matt.*, **11** (1999) R85.
- [6] ANGELL C., NGAI K., MCKENNA G., McMILLAN P. and MARTIN S., *J. Appl. Phys.*, **88** (2000) 3113.
- [7] KISLIUK A., MATHERS R. and SOKOLOV A., *J. Polym. Sci. B: Poly. Phys.*, **38** (2000) 2785.
- [8] GLOTZER S., *J. Non-Cryst. Solids*, **274** (2000) 342.

- [9] BINDER K., BASCHNAGEL J. and WOLFGANG P., *Prog. Polym. Sci.*, **28** (2003) 115.
- [10] KAMATH S., COLBY R. and KUMAR S., *J. Chem. Phys.*, **116** (2002) 865.
- [11] LAČEVIĆ N., STARR F., SCHRÖDER T., NOVIKOV V. and GLOTZER S., *Phys. Rev. E*, **66** (2002) 030101.
- [12] JOHNSON G., MELCUK A., GOULD H., KLEIN W. and MOUNTAIN R., *Phys. Rev. E*, **57** (1998) 5707.
- [13] GLOTZER S. and DONATI C., *J. Phys: Condens. Matter*, **11** (1999) A285.
- [14] GIOVAMBATTISTA N., BULDYREV S., STARR F. and STANLEY H., *Phys. Rev. Lett.*, **90** (2003) 085506.
- [15] DONATI C., DOUGLAS J., KOB W., PLIMPTON S., POOLE P. and GLOTZER S., *Phys. Rev. Lett.*, **80** (1998) 2338.
- [16] DONATI C., GLOTZER S., POOLE P., KOB W. and PLIMPTON S., *Phys. Rev. E*, **60** (1999) 3107.
- [17] MURANAKA T., *Prog. Theor. Phys. Supp.*, **138** (2000) 217.
- [18] KAMATH S., *Doctoral dissertation* (Pennsylvania State University) 2003.
- [19] MEL'CUK A., RAMOS R., GOULD H., KLEIN W. and MOUNTAIN R., *Phys. Rev. Lett.*, **75** (1995) 2522.
- [20] COLBY R., *Phys. Rev. E*, **61** (2000) 1783.
- [21] ERWIN B. and COLBY R., *J. Non-Cryst. Solids*, **307-310** (2002) 225.
- [22] STICKEL F., FISCHER E. and RICHERT R., *J. Chem. Phys.*, **105** (1996) 2043.
- [23] WOLFGARDT M., BASCHNAGEL J., PAUL W. and BINDER K., *Phys. Rev. E*, **54** (1996) 1535.
- [24] BASCHNAGEL J., WOLFGARDT M., PAUL W. and BINDER K., *J. Res. Nat. Inst. Stand. Tech.*, **102** (1997) 159.
- [25] ZHANG W., ZOU X., JIN A. and TIAN D., *Phys. Rev. E*, **61** (2000) 2805.
- [26] REINSBERG S., HEUER A., DOLIWA B., ZIMMERMANN H. and SPIESS H., *J. Non-Cryst. Solids*, **307-310** (2002) 208.
- [27] QIU X. and EDIGER M., *J. Phys. Chem. B*, **107** (2002) 459.
- [28] BÖHMER R., NGAI K., ANGELL C. and PLAZEK D., *J. Chem. Phys.*, **99** (1993) 4201.
- [29] WAGNER H. and RICHERT R., *J. Non-Cryst. Solids*, **242** (1998) 19.
- [30] CHANG I. and SILLESCU H., *J. Phys. Chem. B*, **101** (1997) 8794.
- [31] STICKEL F., *Doctoral dissertation* (Mainz University) 1995.
- [32] HEUBERGER G. and SILLESCU H., *J. Chem. Phys.*, **100** (1996) 15255.
- [33] NAKHELI A., ELJAZOULI A., ELMORABIT M., BALLOUKI E., FORNAZERO J. and HUCK J., *J. Phys: Condens. Matter*, **11** (1999) 7977.
- [34] NOZAKI R., SUZUKI D., OZAWA S. and SHIOZAKI Y., *J. Non-Cryst. Solids*, **235-237** (1998) 393.
- [35] NAOKI M. and KASHIMA S., *J. Phys. Chem.*, **97** (1993) 12356.
- [36] CICERONE M., BLACKBURN F. and EDIGER M., *J. Chem. Phys.*, **102** (1995) 471.
- [37] PLAZEK D., BERO C. and CHAY I., *J. Non-Cryst. Solids*, **172-174** (1994) 181.
- [38] FUJARA F., GEIL B., SILLESCU H. and FLEISCHER G., *Z. Phys. B*, **88** (1992) 195.
- [39] GREET R. and TURNBULL D., *J. Chem. Phys.*, **46** (1967) 1243.
- [40] CUKIERMAN M. and UHLMANN D., *J. Non-Cryst. Solids*, **12** (1973) 199.
- [41] LAUGHLIN W. and UHLMANN D., *J. Phys. Chem.*, **76** (1972) 2317.
- [42] SCHRÖTER K. and DONT H., *J. Chem. Phys.*, **113** (2000) 9101.
- [43] BAINBRIDGE D. and EDIGER M., *Rheol. Acta*, **36** (1997) 209.
- [44] EDWARD J., *J. Chem. Educ.*, **47** (1970) 261.